

Simulation of Cyclic Direct Simple Shear Loading Response of Soils Using Discrete Element Modeling



15 WCEE
LISBOA 2012

A. Dabeet, D. Wijewickreme, & P. Byrne

University of British Columbia, Vancouver, Canada

SUMMARY:

The Direct Simple Shear (DSS) test is one of the laboratory element testing devices that has been widely used to assess soil behavior. Although the DSS test is considered to simulate the cyclic shear loading mode from the earthquakes in an effective manner, the most commonly used versions of the test device (such as the NGI-type DSS device) do not provide means of measuring the lateral stresses on the specimen. This, in turn, results in an inability to define the complete stress state during DSS testing. In recognition of this, along with the need to model soil behavior, numerical modeling of the laboratory element DSS testing process was undertaken using a discrete element method (DEM). The research work presented in this paper indicates that DEM simulations can effectively capture the cyclic shear behavior, including excess pore water pressure generation, observed in laboratory constant volume DSS testing of sands.

Keywords: Discrete Element Method; Direct Simple Shear Test; Cyclic loading.

1. INTRODUCTION

The direct simple shear (DSS) test has been widely used to characterize soil behavior particularly under seismic loading conditions (Bjerrum & Landva 1966; Ishihara & Yamazaki 1980; Wood & Budhu 1980; Finn et al. 1982; Wijewickreme et al. 2005; Kammerer 2006). The key reasons for the growing interest in the DSS test have been due to its simplicity and its ability to more realistically simulate field stress conditions that involve rotation of principal stresses.

A schematic cross section through a typical DSS specimen and the mode of shearing are illustrated in Fig. 1.1 (where: τ , is the horizontal shear stress, σ_v , is the vertical stress and γ , is the shear strain). There are two commonly used types of the DSS test: the Cambridge test type that can accommodate rectangular soil specimens (Roscoe 1953) and the NGI-test type (Bjerrum & Landva 1966) that uses cylindrical shape specimens confined laterally by a wire-reinforced rubber membrane. The NGI-DSS test is the subject of analysis in this paper.

Although the DSS test is experimentally simple to perform, interpretation of test results has not been straightforward partly because radial stresses acting on the reinforced membrane wall are not usually measured. Only a few researchers reported measurements of average radial stress acting on the DSS wire-reinforced membrane in the NGI-DSS device (Youd & Croven 1975; Dyvik et al. 1981; Budhu 1985). Accordingly, the complete stress state of the tested specimen is typically not known, and in turn, this limits the use of the DSS test results for validation of soil constitutive models.

Considering the uncertainties in interpreting DSS testing results as discussed above and in recognition of the common use of the test under cyclic loading conditions, there is a need for analysis of cyclic DSS testing with emphasis on the distribution of radial stresses acting on the perimeter of the specimen's cylindrical wall and along the specimen height. Prevost & Hoeg (1976) and Dounias & Potts (1993) presented the results from analysis of DSS testing based on a continuum approach. With the recent advances in computers, it is now possible to model soil particles more realistically using the discrete element method (DEM) (Cundall & Strack 1979). DEM provides an opportunity to estimate stress conditions at a given zone in a DSS specimen in addition to those obtainable from average boundary measurements. In essence, it is an ideal analysis tool for investigating

the distribution of stresses within simulated soil specimens. In this study, a cylindrical DSS specimen subjected to cyclic loading was analyzed using discrete element modeling (PFC3D 3.1 particle flow code in three dimensions developed by Itasca), and this paper presents some key findings from this work with emphasis on the development radial stresses during cyclic loading.

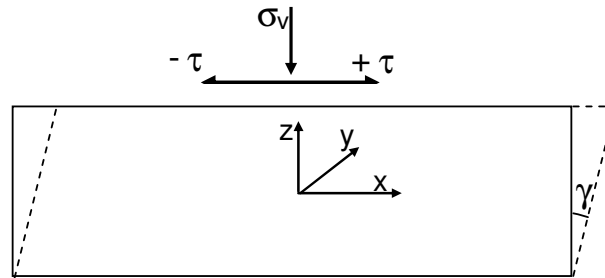


Figure 1.1. Schematic showing a cross-section through the DSS specimen parallel to the direction of shearing.
Note: τ , = horizontal shear stress; σ_v = vertical stress; and γ = shear strain.

2. PFC3D-DSS MODEL DESCRIPTION

Particle Flow Code in three dimensions (PFC3D) is based on the discrete elements method by Cundall & Strack (1979) and Itasca (2005b). Soil particles are modeled as rigid spheres (referred to as balls). The contacts between balls are modeled using the soft contacts approach that allows particle to virtually overlap (Itasca 2005a). The magnitude of the overlap is related to the forces at the contacts through normal and shear stiffness values, K_n and K_s , respectively. Identical values were used for K_n and K_s parameters in this paper. Accordingly, stiffness parameter, K , was used to refer to both shear and normal stiffness at the contacts. These stiffness values have the units of force/displacement. Maximum friction, F , at the contacts can be specified. Slippage occurs if the ratio of shear to normal forces exceeds maximum friction. Boundaries are referred to as walls. The contacts between the balls and walls are modeled in a similar way to contacts between balls. The code uses an explicit solution scheme. Continuum quantities such as stresses can be computed by averaging forces at contacts over an area of interest.

The discrete element method, and PFC3D, in particular have been increasingly used in modeling soils (Cheng et al. 2003; Powrie et al. 2005; Dabeet et al. 2010). The capability of the PFC code for simulating the direct simple shear apparatus has already been demonstrated by the authors (Dabeet et al. 2011) by comparing the DSS response patterns of spherical granular particles using PFC modeling with those obtained from laboratory DSS testing carried out on air-pluviated glass beads. Dabeet et al. (2011) noted that observed good agreement of the shear response between PFC modeling and experiments highlights the potential of discrete element modeling to effectively capture the behavior of granular materials. As such, the use of PFC modeling is considered reasonable for the present investigation.

The selected values for contact model input parameters, K and F , for the simulations herein were 500 kN/m and 0.2, respectively. These values were selected based on the findings of Dabeet et al. (2011) and comparison with the results of one cyclic DSS test on Fraser River sand as will be discussed in the following section. A specific gravity for the simulated balls of 2.5 was used. Viscous damping with a damping ratio of 0.7 was used. The results of the simulations were fairly insensitive to the selected damping ratio as these simulations were performed under pseudo-static (very slow) cyclic loading conditions.

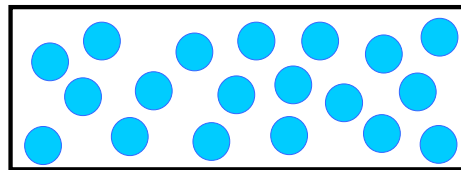
A DSS specimen with a height of 2.1 cm and a diameter of 7 cm filled with “balls” was considered for the PFC simulations herein, leading to a typical height to diameter ratio of 0.3. In the simulations reported in this paper, the balls were first randomly generated inside the specimen cavity with an initial ball diameter smaller than their intended final diameter. The diameter of the balls was then numerically increased to the final diameter for the analysis and contacts between adjacent particles are formed. The particle assembly formation is illustrated in Fig. 2.1. Fig. 2.1a shows the generated balls with an initial diameter smaller than their intended final diameter. The final assembly is shown in Fig. 2.1b after particle expansion (i.e. increase in particles diameter). The final assembly of balls has uniform particles with a selected diameter of 2 mm. The number of generated balls to fill the specimen size is around 10,000. The selected particles diameter and number of particles resulted in a

reasonable computation time. The specimen is bounded laterally by a cylindrical wall that consists of 1.5-mm thick rigid rings. During shearing, the rings are moved independently at different rates to achieve uniform boundary shear strain, γ . The top and bottom boundaries are simultaneously displaced horizontally as a function of shear strain in the positive and negative x-directions, respectively (see Fig. 1.1 for x-y-z directions).

Consolidation of the simulated specimen was performed by displacing the top and bottom boundaries in the negative and positive z-direction, respectively, to achieve a desired vertical effective stress, σ'_v , value of 100 kPa. Fig. 2.2 is a central cross section through the simulated specimen showing balls and contact forces as black lines (force chains). The thickness of the lines is proportional to the magnitude of contact forces. Force chains seem to be distributed evenly across the specimen which suggests a fairly uniform stress distribution at the end of consolidation and prior to shearing. The achieved void ratio of the particles assembly at the end of consolidation was 0.67.

During cyclic shearing, a constant volume condition was enforced by fixing the top and bottom boundaries of the simulated specimen in the z-direction. It has been shown that the decrease (or increase) in vertical stress acting on the top and bottom boundaries is equivalent to increase (or decrease) in pore water pressure during an undrained test (Finn et al. 1978; Dyvik et al. 1987).

a)



b)

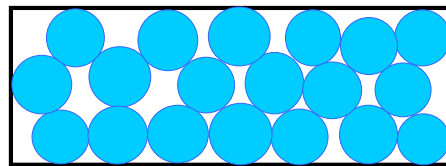


Figure 2.1. Schematic illustrating numerically simulated sample preparation by particle expansion: a) after particle generation and before particle expansion; and b) after particle expansion.

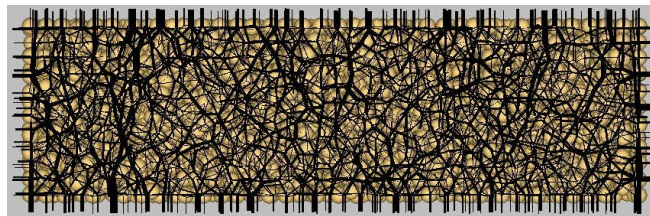


Figure 2.2. A central cross section through the simulated DSS specimen parallel to the x-axis showing contact forces at the end of consolidation and prior to shearing.

3. MODEL RESULTS AND DISCUSSION

3.1. Cyclic loading response

Fig. 3.1 presents typical stress path and stress strain response for a simulation with cyclic stress ratio (CSR= τ_{cy}/σ'_v) of 0.08 and vertical effective stress (σ'_v) of 100 kPa. A gradual drop of vertical effective stress is observed from its initial value of 100 kPa with the application of cyclic shear until it reaches σ'_v value of about 50

kPa followed by a sudden overall drop of σ'_v during the last two cycles. This is associated with the development of relatively large shear strains during the last two cycles of loading.

Fig. 3.2 shows stress path and stress strain response from a typical laboratory cyclic DSS test on loose (relative density, D_r , of 40%) air-pluviated Fraser River sand for a CSR value of 0.08 and σ'_v of 100 kPa reported in Wijewickreme et al. (2005). Similar response of gradual drop in vertical effective σ'_v stress associated with the development of relatively small shear strains at the beginning of cyclic shearing to that in Fig. 3.1 was observed. Dramatic increase in cyclic shear strain occurs in the last loading cycle. This suggests the suitability of the selected model parameters of $K= 500$ kN/m and $F=0.2$ and the discrete element modeling approach utilized to simulate the cyclic behavior as observed from laboratory DSS testing of Fraser River sand in Fig. 3.2.

3.2. Cyclic resistance

For comparison purposes, the cyclic shear resistance herein is defined as the number of load cycles required to reach a single-amplitude horizontal shear strain $\gamma = 3.75\%$, in a given constant volume DSS test under a given applied CSR. This $\gamma = 3.75\%$ condition in a DSS specimen is essentially equivalent to reaching a 2.5% single-amplitude axial strain in a triaxial soil specimen. An identical definition has been previously used to assess the cyclic shear resistance of sands by the U.S. National Research Council (NRC 1985), and it also has been adopted in many previous liquefaction studies at the University of British Columbia.

The instance of reaching $\gamma = 3.75\%$ for the above simulated and laboratory tests are denoted by the dots on the stress-strain and stress path plots shown in Fig. 3.1 and Fig. 3.2, respectively.

Fig. 3.3 presents the cyclic stress ratio plotted against the number of cycles to reach $\gamma = 3.75\%$ obtained from the results of four cyclic simulations with CSR values of 0.06, 0.08, 0.1, and 0.12 (Note: all the simulations were done with the model parameters of $K= 500$ kN/m and $F = 0.2$ which were derived from one calibration to obtain a good agreement with data from one of the laboratory cyclic DSS test as shown in Fig. 3.1 and Fig. 3.2). The results of laboratory cyclic constant volume DSS tests conducted on loose air-pluviated Fraser River sand reported in Wijewickreme et al. (2005) are plotted on the same figure. Good agreement between the trends of cyclic shear resistance obtained for the simulations and the laboratory tests further indicates the suitability of the modeling approach used here for simulating the cyclic behavior of sands.

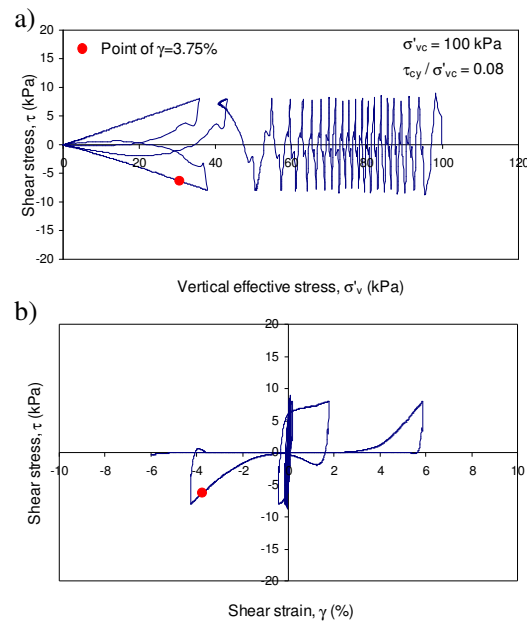


Figure 3.1. Results from numerical simulation of cyclic shear DSS loading of a granular material with CSR (τ_{cy}/σ'_{vc}) of 0.08: a) stress path; and b) shear stress-strain response.

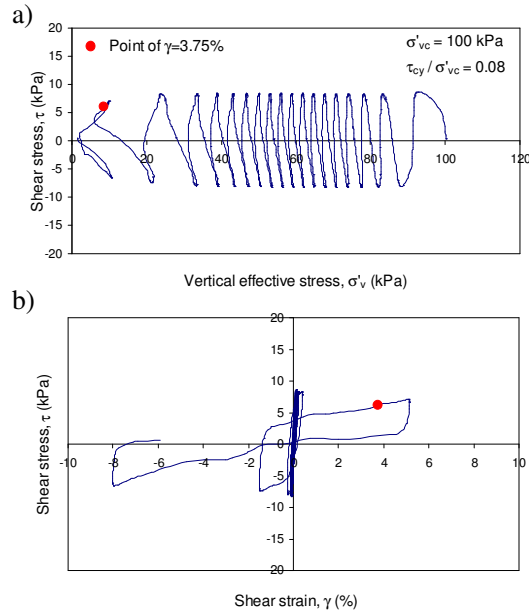


Figure 3.2. Results from cyclic laboratory DSS testing of Fraser River sand for CSR (τ_{cy}/σ'_{vc}) of 0.08: a) stress path; and b) shear stress-strain response (Wijewickreme et al. 2005).

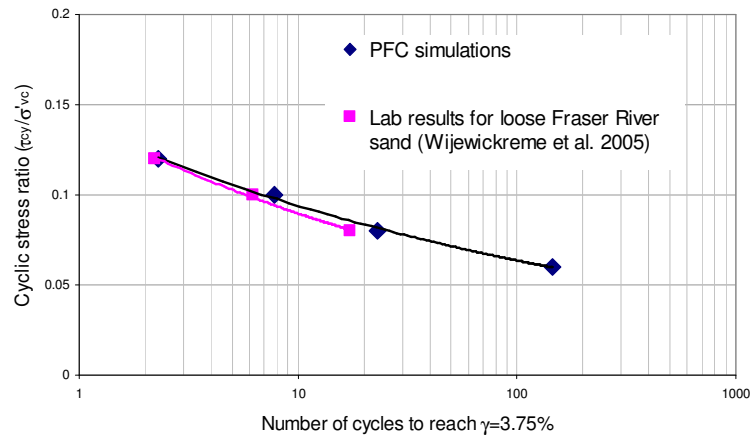


Figure 3.3. Comparison of cyclic resistance obtained from numerical simulation and laboratory testing.

3.3. Lateral stress

The vertical stress path, stress-strain response, and radial stress path for a simulation with cyclic stress ratio (CSR) of 0.12 and $\sigma'_v = 100$ kPa is shown in Fig. 3.4. Vertical effective stress is observed to decrease rapidly with cyclic shearing as it drops momentarily to a value close to zero in about two cycles. Relatively large shear strains develop at the end of the second loading cycle. Radial stress, calculated from particles contact forces acting on the rings surrounding the specimen and averaged over the surface area of the rings, shows an overall drop over the loading cycles from an initial value of about 65 kPa to a value close to zero during the third loading cycle. Due to the soil's tendency to dilate, radial stress increases to about 40kPa during loading parts of the last cycle of shearing. This is followed by a rapid drop of radial stress to a value close to zero during the unloading parts of the cycle.

The development of lateral stress coefficient ($k = \text{Vertical effective stress, } \sigma'_v / \text{radial effective stress, } \sigma'_r$) with the progression of cyclic shearing is shown in Fig. 3.5 plotted against vertical effective stress. The values of

lateral stress coefficient were calculated by normalizing radial stresses shown in Fig. 3.4c by the corresponding values of vertical stress in Fig. 3.4a. At the end of consolidation and before the application of cyclic shear stress, lateral stress coefficient at rest (k_0) has a value of 0.65. It is noted that this value from numerical computations is higher than the value of about ~ 0.5 expected for Fraser River sand. The value of k_0 is particularly dependent on the selected F parameter for numerical modeling. It appears that the chosen value of $F = 0.2$ for getting a good match in the shear response has not been able to capture the lateral stress under k_0 conditions. It should be noted that k values calculated in the vicinity of zero vertical effective stress are not reliable due the potential for large errors in the calculation at small stresses.

In spite of these limitations, the numerical modeling still provides a pathway to examine the variation of k during a cyclic shear test as shown in Fig. 3.5. An overall trend of increase in lateral stress coefficient is observed with the progression of cyclic loading. A maximum k value of about 1.00 was calculated at the end of cyclic shearing. These results are in qualitative agreement with the experimental findings of Youd & Croven (1975) and Budhu (1985) that showed an overall increase in lateral stress coefficient with the increase in the number of shearing cycles.

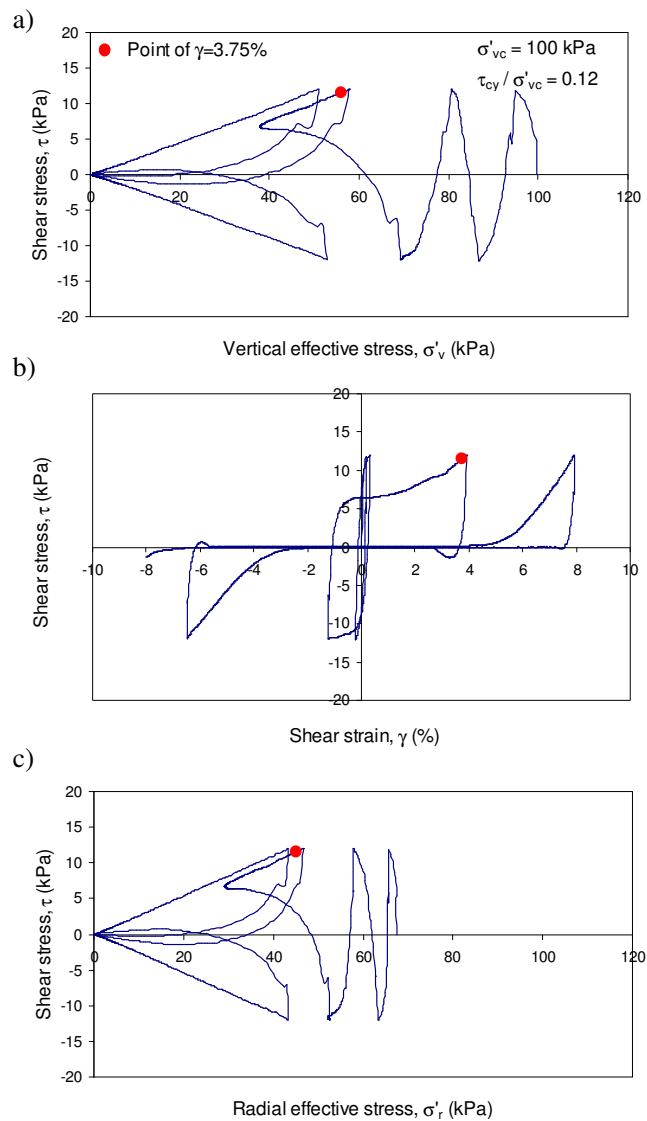


Figure 3.4. Simulation results for CSR (τ_{cy}/σ'_{vc}) of 0.12. a) vertical stress path; b) shear stress-strain response; and c) radial stress path.

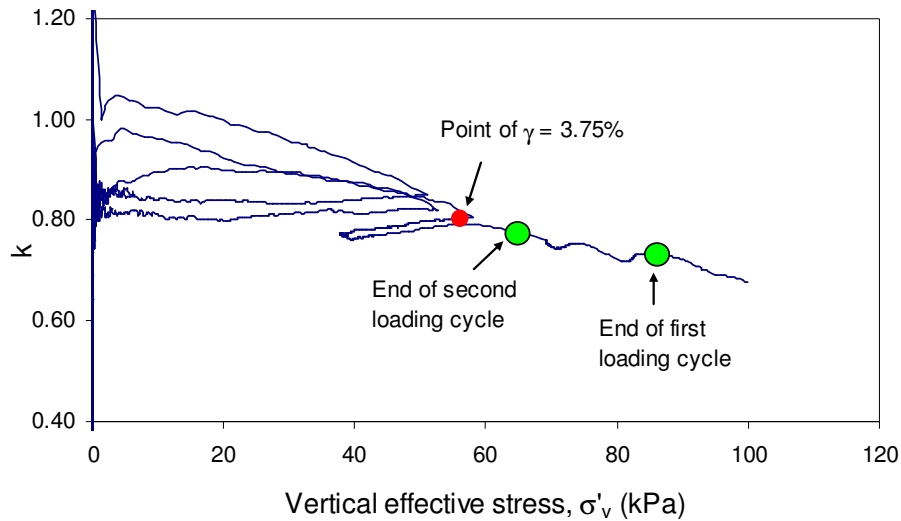


Figure 3.5. Lateral stress coefficient ($k=\sigma'_h/\sigma'_v$) plotted against σ'_v for the simulation with CSR of 0.12 shown in Fig. 3.4.

4. CONCLUSIONS

The Direct Simple Shear (DSS) test is one of the laboratory element testing devices that has been widely used to assess soil behavior, particularly in response to earthquakes loading. The performance of an NGI-type DSS specimen filled with spherical particles under constant volume cyclic shearing was simulated using PFC3D based on the Discrete Element Method (DEM). The model was calibrated using the stress strain behavioral patterns available from one of the laboratory cyclic DSS tests conducted at the University of British Columbia on Fraser River sand.

It was found that, with appropriate selection of model parameters, the DEM approach is able to effectively capture the cyclic shear behavior, including excess pore water pressure generation, observed in laboratory constant volume DSS testing of sands. Very good agreement was noted between the trends of cyclic shear resistance obtained from the DEM simulations and those from laboratory tests further reinforcing the suitability of the modeling approach.

Although the DSS test is considered to simulate the cyclic shear loading mode from the earthquakes in an effective manner, the most commonly used NGI-type DSS device does not provide means of measuring the lateral stresses on the specimen. On the other hand, the DEM modeling also provided an opportunity to examine the development of lateral stresses during cyclic loading. Lateral stress coefficient, starting from an at-rest state, was noted to increase with the increase of the number of cycles to a value of about 1.00 towards the end of cyclic shearing at relatively large shear strains. These results are in qualitative agreement with previous experimental findings that have shown an overall increase in lateral stress coefficient with the increase in the number of shearing cycles.

REFERENCES

- Bjerrum, L. and Landva, A. (1966). Direct Simple-Shear Tests on a Norwegian Quick Clay. *Géotechnique*. **16:1**, 1-20.
- Budhu, M. (1985). Lateral Stresses Observed in Two Simple Shear Apparatus. *Journal of Geotechnical Engineering*. **111:6**, 698-711.
- Cheng, Y.P., Bolton, M.D., and Nakata, Y. (2003). Discrete element simulation of crushable soil. *Géotechnique*. **53:7**, 633-641.
- Cundall, P.A. and Strack, O.D.L. (1979). A discrete numerical model for granular assemblies. *Géotechnique*. **29:1**, 47-65.

- Dabeet, A., Wijewickreme, D., and Byrne, P. (2010). Evaluation of the stress-strain uniformities in the direct simple shear device using 3D discrete element modeling. *63rd Canadian Geotechnical Conference*. Calgary.
- Dabeet, A., Wijewickreme, D. and Byrne, P. (2011). Discrete element modeling of direct simple shear response of granular soils and model validation using laboratory element tests. *14th Pan-Am. Conference and 64th Canadian Geotechnical conference*. Toronto.
- Dounias, G.T., and Potts, D.M. (1993). Numerical Analysis of Drained Direct and Simple Shear Tests. *Journal of Geotechnical Engineering*, **119:12**, 1870-1891.
- Dyvik, R., Berre, T., Lacasse, S., and Raadim, B. (1987). Comparison of truly undrained and constant volume direct simple shear tests. *Géotechnique*. **37:1**, 3-10.
- Dyvik, R., Zimmie, T.F., and Floess, C.H.L. (1981). Lateral stress measurements in Direct Simple Shear Device. *Laboratory Shear Strength of Soils*. ASTM International, 191-206.
- Finn, W.D.L, Vaid, Y.P., and Bhatia, S.K. (1978). Constant volume simple shear testing. *The Second International Conference on Microzonation for Safer Construction-Research and Application*, San Francisco, Calif., 839-851.
- Finn, W.D.L., Bhatia, S.K., and Pickering, D.J. (1982). The cyclic simple shear test. In *Soil Mechanics-Transient and Cyclic Loads*. John Wiley & Sons Ltd., 583-607.
- Ishihara, K., and Yamazaki, F. (1980). Cyclic simple shear tests on saturated sand in multi-directional loading. *Soils and Foundations*. **20:1**, 45-59.
- Itasca Consulting Group. (2005a). PFC3D (Particle Flow Code in Three Dimensions) version 3.1.
- Itasca Consulting Group. (2005b). *PFC3D user manual*, Monneapolis, USA.
- Kammerer, A.M. (2006). Undrained response of Monterey 0/30 sand under multidirectional cyclic simple shear loading conditions. PhD Thesis, University of California, Berkeley.
- NRC. (1985). Liquefaction of soils during earthquakes. National Academic Press, Washington, D.C. National Research Council Report CETS-EE-001.
- Powrie, W. Ni, Q., Harkness, R., and Zhang, X. (2005). Numerical modelling of plane strain tests on sands using a particulate approach. *Géotechnique*. **55**, 297-306.
- Prevost, J. and Hoeg, K. (1976). Reanalysis of simple shear soil testing. *Canadian Geotechnical Journal*. **13**, 418-429.
- Roscoe, K. (1953). An apparatus for the application of simple shear to soil samples. *3rd International Conference on Soil Mechanics*. Zurich, 186-191.
- Wijewickreme, D., Sriskandakumar, S., and Byrne, P. (2005). Cyclic loading response of loose air-pluviated Fraser River sand for validation of numerical models simulating centrifuge tests. *Canadian Geotechnical Journal*. **42:2**, 550-561.
- Wood, D., and Budhu, M. (1980). The behavior of Leighton Buzzard sand in cyclic simple shear tests. *International Symposium on Soils under Cyclic and Transient Loading*. Rotterdam: A. A. Balkema, 9-21.
- Youd, T.L., and Croven, T.N. (1975). Lateral stresses in sands during cyclic loading. *Journal of Geotechnical and Geoenvironmental Engineering*, **101:2**, 217-221.